Title
Exact Transport Representations of the Classical and Nonclassical Simplified PN Equations

Journal
Journal of Computational and Theoretical Transport, 47(4-6)

ISSN
0041-1450

Authors
Makine, I
Vasques, R
Slaybaugh, RN

Publication Date
2018-09-19

DOI
10.1080/23324309.2018.1496938

Peer reviewed

LTTY#1496938, VOL 0, ISS 0

Exact Transport Representations of the Classical and Nonclassical Simplified P_N Equations

I. Makine, R. Vasques, and R.N. Slaybaugh

QUERY SHEET

This page lists questions we have about your paper. The numbers displayed at left can be found in the text of the paper for reference. In addition, please review your paper as a whole for correctness.

Q1. A disclosure statement reporting no conflict of interest has been inserted. Please correct if this is inaccurate.

TABLE OF CONTENTS LISTING

The table of contents for the journal will list your paper exactly as it appears below:

Exact Transport Representations of the Classical and Nonclassical Simplified P_N Equations
I. Makine, R. Vasques, and R.N. Slaybaugh

JOURNAL OF COMPUTATIONAL AND THEORETICAL TRANSPORT
https://doi.org/10.1080/23324309.2018.1496938

Taylor & Francis
Taylor & Francis Group

ARTICLE

Exact Transport Representations of the Classical and Nonclassical Simplified P_N Equations

I. Makine[a,b], R. Vasques[c], and R.N. Slaybaugh[d]

[a]Ecole Polytechnique de Bruxelles, ULB, Bruxelles, Belgium; [b]INSTN, Centre CEA de Saclay, Gif-sur-Yvette, France; [c]Department of Mechanical and Aerospace Engineering, The Ohio State University, Columbus, OH, USA; [d]Department of Nuclear Engineering, University of California, Berkeley, 4151 Etcheverry Hall, Berkeley, CA, USA

ABSTRACT

We show that the recently introduced nonclassical simplified P_N equations can be represented exactly by a nonclassical transport equation. Moreover, we validate the theory by showing that a Monte Carlo transport code sampling from the appropriate nonexponential free-path distribution function reproduces the solutions of the classical and nonclassical simplified P_N equations. Numerical results are presented for four sets of problems in slab geometry.

KEYWORDS

Diffusion equation; transport equation; nonclassical transport; Monte Carlo method

1. Introduction

A *nonclassical* linear Boltzmann equation has been recently proposed (Larsen 2007; Larsen and Vasques 2011) to address transport problems in which the particle flux is not attenuated exponentially. The original motivation for this formulation came from measurements of photon free-paths in atmospheric clouds, which could not be explained by classical radiative transfer with exponential attenuation (cf. sections 5.1 and 8.3 in Davis and Marshak 2010) This theory has since been extended and has found applications for neutron transport in reactor cores (cf. Vasques and Larsen 2014) as well as image rendering in computer graphics (cf. d'Eon 2013).

The nonclassical theory requires the use of a *memory variable*, namely the free-path s, representing the distance traveled by a particle since its previous interaction (birth or scattering). Assuming that scattering is isotropic, the one-speed nonclassical transport equation with an isotropic internal source is written as (Larsen and Vasques 2011)

CONTACT: R. Vasques vasques.4@osu.edu Department of Mechanical and Aerospace Engineering, The Ohio State University, Columbus, OH, USA

$$\frac{\partial \psi}{\partial s} + \mathbf{\Omega} \cdot \nabla \psi + \Sigma_t(s)\psi = \frac{\delta(s)}{4\pi}\left[c\int_{4\pi}\int_0^\infty \Sigma_t(s')\psi\left(x, \mathbf{\Omega}', s'\right)ds'd\Omega' + Q(x)\right]. \tag{1}$$

Here, $\psi = \psi(x, \mathbf{\Omega}, s)$ represents the nonclassical angular flux, c is the scattering ratio, and $Q(x)$ is the source. The total cross section Σ_t is a function of s such that the free-path probability distribution function

$$p(s) = \Sigma_t(s)\mathrm{e}^{-\int_0^s \Sigma_t(s\prime)ds\prime} \tag{2}$$

does not have to be exponential.

Equation (1) is a generalization of the linear Boltzmann equation; *classical* transport is recovered when Σ_t is independent of s. In that case, Equation (2) becomes the exponential decay

$$p(s) = p_c(s) := \Sigma_t \mathrm{e}^{-\Sigma_t s}, \tag{3}$$

and Equation (1) reduces to the well-known (classical) one-speed linear Boltzmann equation (Larsen and Vasques 2011)

$$\mathbf{\Omega} \cdot \nabla \Psi(x, \mathbf{\Omega}) + \Sigma_t \Psi(x, \mathbf{\Omega}) = \frac{1}{4\pi}\left[c\int_{4\pi} \Sigma_t \Psi\left(x, \mathbf{\Omega}'\right)d\Omega' + Q(x)\right] \tag{4}$$

for the classical angular flux

$$\Psi(x, \mathbf{\Omega}) = \int_0^\infty \psi(x, \mathbf{\Omega}, s)ds. \tag{5}$$

The simplified P_N ($\mathrm{SP_N}$) equations, first derived by Gelbard (1960, 1961, 1962), have been shown to be a high-order asymptotic approximation of the transport equation (Larsen, Morel, and McGhee 1993). They are particularly attractive when addressing problems in which the spatial and angular dependence of the angular flux is not severe. They are used to improve the quality of transport physics in a diffusion model while avoiding the complexity of the full P_N (spherical-harmonics) or S_N (discrete-ordinates) equations. Specifically, the $\mathrm{SP_N}$ equations can be implemented directly within a diffusion code, with numerical solutions frequently much more transport-like than diffusion solutions. We refer the reader to (McClarren 2011) for a complete review on $\mathrm{SP_N}$ theory.

It has been shown that certain cases in the hierarchy of the classical SP_N equations ($\mathrm{SP_1}$, $\mathrm{SP_2}$, and $\mathrm{SP_3}$) can be represented exactly by a nonclassical transport equation (Frank et al. 2015). One can obtain explicit expressions for the free-path distribution $p(s)$ and the corresponding $\Sigma_t(s)$ such that Equation (1) can be converted to an integral equation for the scalar flux

$$\Phi(x) = \int_{4\pi} \Psi(x, \mathbf{\Omega}) d\Omega = \int_{4\pi} \int_0^\infty \psi(x, \mathbf{\Omega}, s) ds d\Omega \tag{6}$$

that is identical to the integral formulation of the SP_N equations. This result was later extended to include the case of nonclassical diffusion (Vasques 2016).

In this work, the following original results are presented:

1. We demonstrate that the *nonclassical* simplified P_N equations recently introduced in (Vasques and Slaybaugh 2017) are special cases of the nonclassical Boltzmann equation (1). In particular, we derive explicit expressions for $p(s)$ and $\Sigma_t(s)$ such that the nonclassical simplified P_2 and P_3 equations can be exactly represented by a nonclassical transport equation. This fully generalizes the results introduced in (Frank et al. 2015; Vasques 2016). (This result has been shown for the nonclassical simplified P_1 in Vasques (2016)).
2. We show that the moments of the transport free-path distribution $p(s)$ are approximated with increasing accuracy as the order of the SP_N equations increases. If $p(s)$ is an exponential, even moments up to $2N$ are exactly preserved.
3. We establish that the sampling of s from the probability function $p(s)$ for this generalized results can be explicitly performed in terms of a computed-generated random number. This allows us to use Monte Carlo methods to solve these equations.
4. We present *for the first time* numerical simulations that validate the theory proposed in references (Frank et al. 2015; Vasques 2016), as well as the generalized theory introduced here. We consider transport in slab geometry and perform Monte Carlo simulations in which the free-paths are sampled from the appropriate nonexponential distributions, demonstrating that they match the solutions obtained with both the classical and the nonclassical forms of the simplified P_N equations. This effectively shows that it is possible to solve diffusion, SP_2, and SP_3 problems using a nonclassical Monte Carlo *transport* method.

The remainder of the paper is organized as follows. In Section 2, we describe the classical and nonclassical simplified P_N equations. A sketch of the integral formulation for Equation (1) is presented in Section 3. In Section 4, we use Green's function analysis to show that the nonclassical simplified P_N equations can be represented as nonclassical transport equations. Section 5 presents the numerical results that validate the theory. The paper concludes with a brief discussion in Section 6.

2 Simplified P_N equations

The nonclassical simplified P_N equations (Nc-SP$_N$) are a set of diffusion approximations to Equation (1) derived by Vasques and Slaybaugh using a high-order asymptotic expansion (Vasques and Slaybaugh 2017). This asymptotic analysis requires the first $2M$ raw moments of the free-path distribution $p(s)$ to be finite in order to obtain the Nc-SP$_N$ equations for $N=M$. Here, we will limit ourselves to presenting the Nc-SP$_1$, Nc-SP$_2$, and Nc-SP$_3$ formulations for the nonclassical transport equation (1).

Let us define

$$\langle s^m \rangle := \int_0^\infty s^m p(s) ds \tag{7}$$

as the mth raw moment of the free-path distribution function $p(s)$. The second-order Nc-SP$_N$ equations are explicitly given as follows (Vasques and Slaybaugh 2017):

(I) Nonclassical simplified P_1 equation (Nc-SP$_1$):

$$-\frac{1}{6}\frac{\langle s^2\rangle}{\langle s\rangle}\nabla^2\Phi(x)+\frac{1-c}{\langle s\rangle}\Phi(x)=Q(x). \tag{8}$$

(II) Nonclassical simplified P_2 equation (Nc-SP$_2$):

$$\begin{aligned}-\frac{1}{6}\frac{\langle s^2\rangle}{\langle s\rangle}\nabla^2\left[\Phi(x)+\lambda_1\left[(1-c)\Phi(x)-\langle s\rangle Q(x)\right]\right]+\\ \frac{1-c}{\langle s\rangle}\left[1-\beta_1(1-c)\right]\Phi(x)=\left[1-\beta_1(1-c)\right]Q(x),\end{aligned} \tag{9}$$

where λ_1 and β_1 are constants given by

$$\lambda_1=\frac{3}{10}\frac{\langle s^4\rangle}{\langle s^2\rangle^2}-\frac{1}{3}\frac{\langle s^3\rangle}{\langle s\rangle\langle s^2\rangle}, \tag{10a}$$

$$\beta_1=\frac{1}{3}\frac{\langle s^3\rangle}{\langle s\rangle\langle s^2\rangle}-1. \tag{10b}$$

(III) Nonclassical simplified P_3 equations (Nc-SP$_3$):

$$-\frac{1}{6}\frac{\langle s^2\rangle}{\langle s\rangle}\nabla^2\left[\left[1+\beta_1(1-c)\right]\Phi(x)+2\nu(x)\right]+\frac{1-c}{\langle s\rangle}\Phi(x)=Q(x), \tag{11a}$$

$$-\frac{1}{6}\frac{\langle s^2\rangle}{\langle s\rangle}\nabla^2\left[\frac{\lambda_1}{2}\Phi(x)+\lambda_2\nu(x)\right]+\frac{1-\beta_2(1-c)}{\langle s\rangle}\nu(x)=0, \tag{11b}$$

where λ_2 and β_2 are constants given by

$$\lambda_2=\frac{1}{10\langle s^2\rangle\langle s^3\rangle-9\langle s\rangle\langle s^4\rangle}\left[\frac{9}{5}\langle s^5\rangle-\frac{27}{21}\frac{\langle s\rangle\langle s^6\rangle}{\langle s^2\rangle}+3\frac{\langle s^3\rangle\langle s^4\rangle}{\langle s^2\rangle}-\frac{10}{3}\frac{\langle s^3\rangle^2}{\langle s\rangle}\right], \tag{12a}$$

$$\beta_2 = \frac{1}{10\langle s^2\rangle\langle s^3\rangle - 9\langle s\rangle\langle s^4\rangle}\left[\frac{10}{3}\frac{\langle s^3\rangle^2}{\langle s\rangle} - \frac{9}{5}\langle s^5\rangle\right] - 1, \tag{12b}$$

and λ_1 and β_1 are given by Equations (10).

The Nc-SP$_N$ equations described in items (I)–(III) above represent a generalization of the classical SP$_N$ equations. If Σ_t is independent of s, then Equation (3) holds and $\langle s^m\rangle = \langle s^m\rangle_c := m!\Sigma_t^{-m}$. Under these circumstances, $\lambda_1 = 4/5, \lambda_2 = 11/7, \beta_1 = \beta_2 = 0$, and the Nc-SP$_N$ equations reduce to the classical formulations as given in (Larsen, Morel, and McGhee 1993):

(IV) Classical simplified P_1 equation (SP$_1$):

$$-\frac{1}{3\Sigma_t}\nabla^2\Phi(x) + (1-c)\Sigma_t\Phi(x) = Q(x). \tag{13}$$

(V) Classical simplified P_2 equation (SP$_2$):

$$-\frac{1}{3\Sigma_t}\nabla^2\left[\Phi(x) + \frac{4}{5}\frac{(1-c)\Sigma_t\Phi(x) - Q(x)}{\Sigma_t}\right] + (1-c)\Sigma_t\Phi(x) = Q(x). \tag{14}$$

(VI) Classical simplified P_3 equations (SP$_3$):

$$-\frac{1}{3\Sigma_t}\nabla^2[\Phi(x) + 2\nu(x)] + (1-c)\Sigma_t\Phi(x) = Q(x), \tag{15a}$$

$$-\frac{1}{3\Sigma_t}\nabla^2\left[\frac{2}{5}\Phi(x) + \frac{11}{7}\nu(x)\right] + \Sigma_t\nu(x) = 0. \tag{15b}$$

The classical SP$_N$ formulations described in items (IV)–(VI) are asymptotic approximations of the classical linear Boltzmann equation (4).

3 Integral equation formulation

In this section, we sketch the derivation of the integral equation formulation for Equation (1). A detailed derivation can be found in (Larsen and Vasques 2011).

Let $S(x)$ be given by

$$S(x) = c\int_{4\pi}\int_0^\infty \Sigma_t(s')\psi(x,\mathbf{\Omega}',s')ds'd\mathbf{\Omega}' + Q(x) = cf(x) + Q(x), \tag{16a}$$

where

$$f(x) = \int_0^\infty \Sigma_t(s')\phi(x,s')ds' = \text{collision}-\text{rate density} \tag{16b}$$

$$\phi(x,s) = \int_{4\pi}\psi(x,\mathbf{\Omega},s)d\mathbf{\Omega} = \text{nonclassical scalar flux}. \tag{16c}$$

Equation (1) can now be written as an initial value problem:

$$\frac{\partial \psi}{\partial s}(x, \mathbf{\Omega}, s) + \mathbf{\Omega} \cdot \nabla \psi(x, \mathbf{\Omega}, s) + \Sigma_t(s)\psi(x, \mathbf{\Omega}, s) = 0, 0<s, \tag{17a}$$

$$\psi(x, \mathbf{\Omega}, 0) = \frac{S(x)}{4\pi}. \tag{17b}$$

Following the work in (Larsen and Vasques 2011) and (Frank et al. 2015), we perform the following steps:

1. Calculate the solution of Equations (17) using the method of characteristics;
2. Operate on this solution by $\int_{4\pi}\int_0^\infty \Sigma_t(s)(\cdot)dsd\mathbf{\Omega}$;
3. Perform a change of spatial variables, from the three-dimensional (3-D) spherical $(\mathbf{\Omega}, s)$ to the 3-D Cartesian $x' = x - s\mathbf{\Omega}$.

This yields

$$f(x) = \int\int\int S(x')\frac{p(|x'-x|)}{4\pi|x'-x|^2}dV', \tag{18}$$

where $p(|x'-x|)$ is given by Equation (2).

For classical transport, $p(s) = p_c(s)$ as given in Equation (3), and

$$f(x) = \int\int\int S(x')\frac{\Sigma_t e^{-\Sigma_t|x'-x|}}{4\pi|x'-x|^2}dV' = \int\int\int \left[cf(x') + Q(x')\right]\frac{\Sigma_t e^{-\Sigma_t|x'-x|}}{4\pi|x'-x|^2}dV'. \tag{19}$$

This is the classical integral equation for the scalar flux obtained from Equation (4). Sampling of s is given by

$$\xi = \int_0^s p_c(s')ds' = 1-e^{-\Sigma_t s} \Rightarrow s = -\frac{1}{\Sigma_t}\ln(1-\xi) = -\frac{1}{\Sigma_t}\ln(\xi). \tag{20}$$

Table 1 presents expressions and numerical values of the first six moments of $p_c(s)$.

4. Exact transport representations of the Nc-SP$_N$ equations

In this section, we perform a Green's function analysis for each of the Nc-SP$_N$ equations described in Section 2. The goal is to convert these equations into an integral equation for the scalar flux $\Phi(x)$. By choosing the appropriate $p(s)$, the integral equation (18) becomes equivalent to the integral formulation obtained by this Green's function analysis. Therefore, using the corresponding $\Sigma_t(s)$, Equation (1) becomes an exact representation of the Nc-SP$_N$ equations.

Table 1. Moments of $p_c(s)$ (classical transport).

Moment	General expression	Numerical value if $\Sigma_t = 1$
$\langle s \rangle_c$	$\frac{1}{\Sigma_t}$	1
$\langle s^2 \rangle_c$	$\frac{2!}{\Sigma_t^2}$	2
$\langle s^3 \rangle_c$	$\frac{3!}{\Sigma_t^3}$	6
$\langle s^4 \rangle_c$	$\frac{4!}{\Sigma_t^4}$	24
$\langle s^5 \rangle_c$	$\frac{5!}{\Sigma_t^5}$	120
$\langle s^6 \rangle_c$	$\frac{6!}{\Sigma_t^6}$	720

4.1 Nc-SP$_1$ equation (diffusion)

This nonclassical result was originally presented in (Vasques 2016) and is included here for completeness. We define

$$S(x) = c\langle s \rangle^{-1}\Phi(x) + Q(x) \tag{21}$$

and rewrite Equation (8) as

$$-\nabla^2\Phi(x) + \alpha^2\Phi(x) = \alpha^2\langle s \rangle S(x), \tag{22}$$

where $\alpha^2 = 6/\langle s^2 \rangle$. The Green's function for the operator $(-\nabla^2 + \alpha^2)$ on the left hand side of Equation (22) is

$$G_{sp_1}\left(|x-x'|\right) = \frac{e^{-\alpha|x-x'|}}{4\pi|x-x'|}. \tag{23}$$

Therefore, we can transform Equation (22) into an integral equation for $\Phi(x)$ by taking

$$\Phi(x) = \int\int\int G_{sp_1}\left(|x-x'|\right)\alpha^2\langle s \rangle S(x')dV' = \int\int\int \frac{\alpha^2\langle s \rangle |x-x'|e^{-\alpha|x-x'|}}{4\pi|x-x'|^2} S(x')dV'. \tag{24}$$

Bearing in mind that $\langle s \rangle$ represents the mean free path of a particle (i.e., the average distance between collisions), the collision-rate density can be written as $f(x) = \langle s \rangle^{-1}\Phi(x)$, such that

$$f(x) = \frac{\Phi(x)}{\langle s \rangle} = \int\int\int \frac{\alpha^2|x-x'|e^{-\alpha|x-x'|}}{4\pi|x-x'|^2} S(x')dV'. \tag{25}$$

This result agrees with Equation (18) if and only if

$$p(s) = p_{sp_1}(s) := \alpha^2 s e^{-\alpha s} = \frac{6se^{-\sqrt{6/<s^2>}s}}{\langle s^2 \rangle}. \tag{26}$$

It is easy to verify that $p_{sp_1}(s)$ is always positive and that $\int_0^\infty p_{sp_1}(s)ds = 1$, which proves that it is a probability density function. The total cross section is given by

$$\Sigma_t(s) = \Sigma_{t,sp_1}(s) := \frac{p_{sp_1}(s)}{\int_s^\infty p_{sp_1}(s')ds'} = \frac{\alpha^2 s}{1+\alpha s}. \tag{27}$$

This shows that the nonclassical Equations (1) and (18) with $p(s) = p_{sp_1}(s)$ and $\Sigma_t(s) = \Sigma_{t,sp_1}(s)$ reproduce the Nc-SP$_1$ equation. We can calculate the mth raw moments of $p_{sp_1}(s)$:

$$\langle s^m \rangle_{sp_1} := \int_0^\infty \frac{6s^{m+1}\mathrm{e}^{-\sqrt{6/<s^2>}s}}{\langle s^2 \rangle} ds = \frac{(m+1)!\langle s^2 \rangle^{m/2}}{6^{m/2}}. \tag{28}$$

If classical transport takes place, the moments in Table 1 hold and

$$p_{sp_1}(s) = 3\Sigma_t^2 s\mathrm{e}^{-\sqrt{3}\Sigma_t s}, \tag{29}$$

which is the probability function derived in (Frank et al. 2015) for the SP$_1$ Equation (13). The total cross section becomes

$$\Sigma_{t,sp_1}(s) = \frac{3\Sigma_t^2 s}{1+\sqrt{3}\Sigma_t s}. \tag{30}$$

Table 2 shows the nonclassical and classical expressions for the moments of $p_{sp_1}(s)$, as well as numerical values of the classical moments when $\Sigma_t = 1$. It can be seen from the general expressions that the second moment of the original transport $p(s)$ is always exactly preserved. Comparing to the classical transport moments $\langle s^m \rangle_c$ (see Table 1), the first moment is slightly overestimated while the remaining higher-order moments are underestimated.

Table 2. Moments of $p_{sp_1}(s)$ (diffusion).

Moment	Nonclassical Expression	Classical Expression	Numerical value If $\Sigma_t = 1$
$\langle s \rangle_{sp_1}$	$\frac{2}{\sqrt{6}}\langle s^2 \rangle^{1/2}$	$\frac{2}{\sqrt{3}\Sigma_t}$	1.1547
$\langle s^2 \rangle_{sp_1}$	$\langle s^2 \rangle$	$\frac{2}{\Sigma_t^2}$	2
$\langle s^3 \rangle_{sp_1}$	$\frac{4}{\sqrt{6}}\langle s^2 \rangle^{3/2}$	$\frac{8}{\sqrt{3}\Sigma_t^3}$	4.6188
$\langle s^4 \rangle_{sp_1}$	$\frac{10}{3}\langle s^2 \rangle^2$	$\frac{40}{3\Sigma_t^4}$	13.3333
$\langle s^5 \rangle_{sp_1}$	$\frac{10\sqrt{6}}{3}\langle s^2 \rangle^{5/2}$	$\frac{80}{\sqrt{3}\Sigma_t^5}$	46.1880
$\langle s^6 \rangle_{sp_1}$	$\frac{70}{3}\langle s^2 \rangle^3$	$\frac{560}{3\Sigma_t^6}$	186.6667

Sampling of s is given by

$$\xi = \int_0^s \alpha^2 s' \mathrm{e}^{-\alpha s'} ds' = 1 - (1+\alpha s)\mathrm{e}^{-\alpha s}$$
$$= 1 - \left[1 + \left(\frac{\sqrt{6}}{\sqrt{\langle s^2\rangle}}\right)s\right] \exp\left[\left(-\frac{\sqrt{6}}{\sqrt{\langle s^2\rangle}}\right)s\right]. \tag{31}$$

Hence,

$$s = \frac{1}{\alpha}\tau^{-1}(\xi) = \frac{\sqrt{\langle s^2\rangle}}{\sqrt{6}}\tau^{-1}(\xi) \tag{32}$$

where

$$\tau(z) = (1+z)\mathrm{e}^{-z}. \tag{33}$$

In the classical case, this expression reduces to (Frank et al. 2015)

$$s = \frac{1}{\sqrt{3}\Sigma_t}\tau^{-1}(\xi). \tag{34}$$

4.2 Nc-SP$_2$ equation

Using the definition in Equation (21), we can rewrite Equation (9) as

$$-\frac{\langle s^2\rangle}{6\langle s\rangle}\nabla^2[(1+\lambda_1)\Phi] + \left[1-\beta_1(1-c)\right]\frac{\Phi}{\langle s\rangle} = \left[1-\beta_1(1-c)\right]S - \frac{\lambda_1}{6}\langle s^2\rangle\nabla^2 S. \tag{35}$$

Let us define a new constant α such that

$$\alpha^2 = \frac{6}{\langle s^2\rangle}\frac{1}{1+\lambda_1}\left[1-\beta_1(1-c)\right]. \tag{36}$$

Multiplying Equation (35) by $6\frac{\langle s\rangle}{\langle s^2\rangle}\frac{1}{1+\lambda_1}$ we obtain

$$-\nabla^2\Phi + \alpha^2\Phi = \alpha^2\langle s\rangle S - \frac{\lambda_1}{1+\lambda_1}\langle s\rangle\nabla^2 S, \tag{37}$$

which can be rewritten as

$$[-\nabla^2 + \alpha^2]\Phi = \frac{1}{\lambda_1+1}\alpha^2\langle s\rangle S + \frac{\lambda_1}{1+\lambda_1}\langle s\rangle(-\nabla^2+\alpha^2)S. \tag{38}$$

The Green's function associated with the operator $(-\nabla^2+\alpha^2)$ is

$$G_{sp_2}(|x-x'|) = \frac{\mathrm{e}^{-\alpha|x-x'|}}{4\pi|x-x'|}. \tag{39}$$

Table 3. Moments of $p_{sp_2}(s)$.

Moment	Nonclassical Expression	Classical Expression	Numerical value If $\Sigma_t = 1$
$\langle s \rangle_{sp_2}$	$\frac{2\sqrt{\langle s^2 \rangle}}{\sqrt{6}\sqrt{1+\lambda_1}\sqrt{1-\beta_1(1-c)}}$	$\frac{\sqrt{20}}{\sqrt{27}\Sigma_t}$	0.8606
$\langle s^2 \rangle_{sp_2}$	$\frac{\langle s^2 \rangle}{1-\beta_1(1-c)}$	$\frac{2}{\Sigma_t^2}$	2
$\langle s^3 \rangle_{sp_2}$	$\frac{4\sqrt{1+\lambda_1}}{\sqrt{6}\sqrt{(1-\beta_1(1-c))^3}}\langle s^2 \rangle^{3/2}$	$\frac{8\sqrt{3}}{\sqrt{5}\Sigma_t^3}$	6.1968
$\langle s^4 \rangle_{sp_2}$	$\frac{10(1+\lambda_1)}{3(1-\beta_1(1-c))^2}\langle s^2 \rangle^2$	$\frac{24}{\Sigma_t^4}$	24
$\langle s^5 \rangle_{sp_2}$	$\frac{10\sqrt{6}(1+\lambda_1)^{3/2}}{3(1-\beta_1(1-c))^{5/2}}\langle s^2 \rangle^{5/2}$	$\frac{144\sqrt{3}}{\sqrt{5}\Sigma_t^5}$	111.5419
$\langle s^6 \rangle_{sp_2}$	$\frac{70(1+\lambda_1)^2}{3(1-\beta_1(1-c))^3}\langle s^2 \rangle^3$	$\frac{3024}{5\Sigma_t^6}$	604.8

Using the Green's function, we can write

$$\Phi(x) = \frac{\alpha^2\langle s \rangle}{1+\lambda_1}\int\int\int G_{sp_2} S dV' + \frac{\lambda_1}{1+\lambda_1}\langle s \rangle S, \tag{40}$$

and the collision-rate density is given by

$$f(x) = \frac{\Phi(x)}{\langle s \rangle} = \frac{\alpha^2}{1+\lambda_1}\int G_{sp_2} S dV' + \frac{\lambda_1}{1+\lambda_1} S. \tag{41}$$

Note that the identity

$$\begin{aligned} S(x) &= \int_0^\infty S(x+s\Omega)\delta(s)ds = \frac{1}{4\pi}\int_{4\pi}\int \delta(s)S(x+s\Omega)dsd\Omega \\ &= \int_{4\pi}\int \frac{\delta(|x-x'|)S(x')}{4|x-x'|^2}dV' \end{aligned} \tag{42}$$

holds, with $x' = x + s\boldsymbol{\Omega}$, $|x-x'| = s$, $s^2 ds d\boldsymbol{\Omega} = dV'$. Therefore, we can rewrite the collision-rate density as

$$f(x) = \frac{\alpha^2}{1+\lambda_1}\int\int\int \frac{|x-x'|e^{-\alpha|x-x'|}}{4\pi|x-x'|^2}S(x')dV' + \frac{\lambda_1}{1+\lambda_1}\int\int\int \frac{\delta(|x-x'|)}{4\pi|x-x'|^2}S(x')dV'. \tag{43}$$

This result agrees with Equation (18) if and only if

$$p(s) = p_{sp_2}(s) := \frac{\alpha^2 s e^{-\alpha s}}{1+\lambda_1} + \frac{\lambda_1}{1+\lambda_1}\delta(s). \tag{44}$$

It is easy to verify that $p_{sp_2}(s)$ is always positive and that $\int_0^\infty p_{sp_2}(s)ds = 1$, proving that it is a probability density function. We can determine the total cross section, which is written as

$$\Sigma_t(s) = \Sigma_{t,sp_2}(s) := \frac{\frac{\lambda_1}{\lambda_1+1}\delta(s) + \alpha^2 s}{1+\alpha s}. \tag{45}$$

The nonclassical Equations (1) and (18) with $p(s) = p_{sp_2}(s)$ and $\Sigma_t(s) = \Sigma_{t,sp_2}(s)$ reproduce the Nc-SP$_2$ equation. We can calculate the mth raw moments of $p_{sp_2}(s)$:

$$\langle s^m \rangle_{sp_2} := \int_0^\infty s^m p_{sp_2}(s) ds = \frac{(m+1)!}{\alpha^m(1+\lambda_1)}. \tag{46}$$

If classical transport takes place, the moments in Table 1 hold and

$$p_{sp_2}(s) = \frac{25}{27}\Sigma_t^2 s e^{-\Sigma_t\sqrt{5/3}s} + \frac{4}{9}\delta(s), \tag{47}$$

which is the probability function derived in (Frank et al. 2015) for the SP$_2$ equation (14). The total cross section becomes

$$\Sigma_{t,sp_2}(s) = \frac{\frac{4}{9}\delta(s) + \frac{5}{3}\Sigma_t^2 s}{1+\sqrt{5/3}\Sigma_t s}. \tag{48}$$

Table 3 shows the nonclassical and classical expressions for the moments of $p_{sp_2}(s)$, as well as numerical values of the classical moments when $\Sigma_t = 1$. The classical moments of $p_{sp_2}(s)$ give a more accurate estimate of the classical transport moments $\langle s^m \rangle_c$ (Table 1) than the ones obtained from $p_{sp_1}(s)$ (Table 2). In particular, both the second and the fourth moments of the original transport $p(s)$ are exactly preserved. However, these moments are *not* generally preserved in the nonclassical case; for instance, the general nonclassical second moment is conserved only if $\beta_1 = 0$.

Sampling of s is given by

$$\xi = \int_0^s p_{sp_2}(s')ds' = \frac{\lambda_1}{1+\lambda_1} + \frac{1}{1+\lambda_1}(1-(1+\alpha s)e^{-\alpha s}). \tag{49}$$

Hence,

$$s = \begin{cases} 0, & \text{for } 0<\xi<\dfrac{\lambda_1}{1+\lambda_1} \\ \dfrac{1}{\alpha}\tau^{-1}\big((\lambda_1+1)(1-\xi)\big), & \text{for } \xi>\dfrac{\lambda_1}{1+\lambda_1} \end{cases}, \tag{50}$$

where $\tau(z)$ is defined in Equation (33). In the classical case, this expression reduces to (Frank et al. 2015)

$$s = \begin{cases} 0, \text{ for } 0<\xi<\dfrac{4}{9} \\ \dfrac{\sqrt{3}}{\sqrt{5}}\dfrac{1}{\Sigma_t}\tau^{-1}\left(\dfrac{9}{5}(1-\xi)\right), \text{ for } \xi>\dfrac{4}{9} \end{cases}. \tag{51}$$

4.3 Nc-SP$_3$ equations

Using the definition in Equation (21), we can rewrite Equations (11) as

$$-\frac{\langle s^2\rangle}{6\langle s\rangle}\nabla^2\left[\left[1+\beta_1(1-c)\right]\Phi+2\nu\right]+\frac{1}{\langle s\rangle}\Phi = S, \tag{52a}$$

$$-\frac{\lambda_2\langle s^2\rangle}{6\langle s\rangle}\nabla^2\nu+\frac{1-\beta_2(1-c)}{\langle s\rangle}\nu = \frac{1}{2}\frac{\lambda_1}{6}\frac{\langle s^2\rangle}{\langle s\rangle}\nabla^2\Phi. \tag{52b}$$

This system can be rewritten as

$$-\frac{\langle s^2\rangle}{6\langle s\rangle}\nabla^2\left[\left[1+\beta_1(1-c)\right]\Phi+2\nu\right]+\frac{1}{\langle s\rangle}\Phi = S, \tag{53a}$$

$$-\frac{\langle s^2\rangle}{6\langle s\rangle}\left(\lambda_2-\frac{\lambda_1}{1+\beta_1(1-c)}\right)\nabla^2\nu+\frac{1-\beta_2(1-c)}{\langle s\rangle}\nu = \frac{1}{2}\frac{\lambda_1}{1+\beta_1(1-c)}\left[\frac{\Phi}{\langle s\rangle}-S\right]. \tag{53b}$$

We need to find the Green's functions associated to this system, which must satisfy

$$-\frac{\langle s^2\rangle}{6\langle s\rangle}\nabla^2\left[\left[1+\beta_1(1-c)\right]G^{\Phi}_{sp_3}+2G^{\nu}_{sp_3}\right]+\frac{1}{\langle s\rangle}G^{\Phi}_{sp_3} = \delta(x), \tag{54a}$$

$$-\frac{\langle s^2\rangle}{6\langle s\rangle}\left(\lambda_2-\frac{\lambda_1}{1+\beta_1(1-c)}\right)\nabla^2G^{\nu}_{sp_3}+\frac{1-\beta_2(1-c)}{\langle s\rangle}G^{\nu}_{sp_3}-\frac{1}{2}\frac{\lambda_1}{1+\beta_1(1-c)}\frac{G^{\Phi}_{sp_3}}{\langle s\rangle} = -\frac{1}{2}\frac{\lambda_1}{1+\beta_1(1-c)}\delta(x). \tag{54b}$$

Here, $G^{\Phi}_{sp_3}$ and $G^{\nu}_{sp_3}$ are functions of $r=|x|$ that enable Equations (53) to be written as

$$\Phi_0(x) = \iiint G^{\Phi}_{sp_3}\left(|x-x'|\right)S(x')dV', \tag{55a}$$

$$\nu(x) = \iiint G^{\nu}_{sp_3}\left(|x-x'|\right)S(x')dV'. \tag{55b}$$

Following the procedure presented in (Frank et al. 2015), we seek $G^{\Phi}_{sp_3}(r)$ and $G^{\nu}_{sp_3}(r)$ that satisfy

$$-\frac{\langle s^2\rangle}{6\langle s\rangle}\frac{1}{r^2}\frac{\partial}{\partial r}r^2\frac{\partial}{\partial r}\left[\left[1+\beta_1(1-c)\right]G^{\Phi}_{sp_3}+2G^{\nu}_{sp_3}\right]+\frac{1}{\langle s\rangle}G^{\Phi}_{sp_3}=0, \tag{56a}$$

$$-\frac{\langle s^2\rangle}{6\langle s\rangle}\left(\lambda_2-\frac{\lambda_1}{1+\beta_1(1-c)}\right)\frac{1}{r^2}\frac{\partial}{\partial r}r^2\frac{\partial}{\partial r}G^{\nu}_{sp_3}+\frac{1-\beta_2(1-c)}{\langle s\rangle}G^{\nu}_{sp_3} -\frac{1}{2}\frac{\lambda_1}{1+\beta_1(1-c)}\left[\frac{G^{\Phi}_{sp_3}}{\langle s\rangle}\right]=0; \tag{56b}$$

with

$$-\frac{\langle s^2\rangle}{6\langle s\rangle}\lim_{\epsilon\to 0}\left[4\pi\epsilon^2\left(\left[1+\beta_1(1-c)\right]\frac{\partial G^{\Phi}_{sp_3}(\epsilon)}{\partial r}+2\frac{\partial G^{\nu}_{sp_3}(\epsilon)}{\partial r}\right)\right]=1, \tag{57a}$$

$$-\frac{\langle s^2\rangle}{6\langle s\rangle}\left(\lambda_2-\frac{\lambda_1}{1+\beta_1(1-c)}\right)\lim_{\epsilon\to 0}\left(4\pi\epsilon^2\frac{\partial G^{\nu}_{sp_3}(\epsilon)}{\partial r}\right)=-\frac{1}{2}\frac{\lambda_1}{1+\beta_1(1-c)}. \tag{57b}$$

Specifically, we are looking for the Green's functions of the form

$$G^{\Phi}_{sp_3}=\frac{e^{-\alpha s}}{4\pi s}, \tag{58a}$$

$$G^{\nu}_{sp_3}=a\frac{e^{-\alpha s}}{4\pi s}, \tag{58b}$$

where α and a are constants to be determined.

Using that $\nabla^2 G^{\Phi}_{sp_3}=\alpha^2 G^{\Phi}_{sp_3}$ and $\nabla^2 G^{\nu}_{sp_3}=\alpha^2 G^{\nu}_{sp_3}$, Equations (56) yield

$$-\frac{\langle s^2\rangle}{6}\left[\left[1+\beta_1(1-c)\right]\alpha^2+2a\alpha^2\right]+1=0, \tag{59a}$$

$$-\frac{\langle s^2\rangle}{6}\left(\lambda_2-\frac{\lambda_1}{1+\beta_1(1-c)}\right)\alpha^2 a+\left(1-\beta_2(1-c)\right)a-\frac{1}{2}\frac{\lambda_1}{1+\beta_1(1-c)}=0. \tag{59b}$$

From Equation (59b) we can determine a, which is given by

$$a=\frac{\frac{1}{2}\frac{\lambda_1}{1+\beta_1(1-c)}}{\left(1-\beta_2(1-c)\right)-\frac{\langle s^2\rangle}{6}\left(\lambda_2-\frac{\lambda_1}{1+\beta_1(1-c)}\right)\alpha^2}. \tag{60}$$

We can now write Equation (59a) as

$$-\frac{\langle s^2\rangle}{6}\left[z_1+\frac{\frac{\lambda_1}{z_1}}{z_2-\frac{\langle s^2\rangle}{6}\left(\lambda_2-\frac{\lambda_1}{z_1}\right)\alpha^2}\right]\alpha^2+1=0, \tag{61}$$

where

$$z_1=1+\beta_1(1-c), \tag{62a}$$

$$z_2 = 1-\beta_2(1-c). \tag{62b}$$

After some manipulations, we attain

$$-\left(\frac{\langle s^2\rangle}{6}\right)^2 z_1\left(\lambda_2-\frac{\lambda_1}{z_1}\right)\alpha^4-\frac{\langle s^2\rangle}{6}(\lambda_2+z_1z_2)\alpha^2+z_2=0. \tag{63}$$

The roots of this polynomial are given by

$$(\alpha^{\pm})^2=\frac{2}{\langle s^2\rangle}\frac{\frac{1}{3}(\lambda_2+z_1z_2)\pm\sqrt{\frac{1}{9}(\lambda_2+z_1z_2)^2-\frac{4}{9}(\lambda_2z_1-\lambda_1)z_2}}{\frac{2}{9}(\lambda_2z_1-\lambda_1)}. \tag{64}$$

Now we can revisit the expression for a; keeping only the non-complex solutions, we have

$$a^{\pm}=\frac{\frac{1}{2}\frac{\lambda_1}{z_1}}{z_2-\frac{3}{2z_1}\left(\frac{1}{3}(\lambda_2+z_1z_2)\pm\sqrt{\frac{1}{9}(\lambda_2+z_1z_2)^2-\frac{4}{9}(\lambda_2z_1-\lambda_1)z_2}\right)}. \tag{65}$$

Thus, we have two solutions of Equations (56): one for α^+ and a^+, and the other for α^- and a^-. The general solution is a linear combination of these two solutions:

$$G^{\Phi}_{sp_3}(s)=\frac{A^+}{\langle s\rangle}\left(\frac{e^{-\alpha^+ s}}{4\pi s}\right)+\frac{A^-}{\langle s\rangle}\left(\frac{e^{-\alpha^- s}}{4\pi s}\right), \tag{66a}$$

$$G^{v}_{sp_3}(s)=\frac{A^+a^+}{\langle s\rangle}\left(\frac{e^{-\alpha^+ s}}{4\pi s}\right)+\frac{A^-a^-}{\langle s\rangle}\left(\frac{e^{-\alpha^- s}}{4\pi s}\right), \tag{66b}$$

where $A^{\pm}$ are determined by Equations (57), such that

$$A^+a^++A^-a^-=\frac{-\lambda_1 3\frac{\langle s\rangle^2}{\langle s^2\rangle}}{\lambda_2z_1-\lambda_1}, \tag{67a}$$

$$A^++A^-=\frac{\left(1+\frac{\lambda_1}{\lambda_2z_1-\lambda_1}\right)}{z_1}6\frac{\langle s\rangle^2}{\langle s^2\rangle}. \tag{67b}$$

Let us define

$$A\prime^+=A^+\frac{\langle s^2\rangle}{3\langle s\rangle^2}, \tag{68a}$$

$$A\prime^-=A^-\frac{\langle s^2\rangle}{3\langle s\rangle^2}, \tag{68b}$$

$$b=\frac{\lambda_1}{\lambda_2z_1-\lambda_1}. \tag{68c}$$

Table 4. Moments of $p_{sp_3}(s)$.

Moment	Classical expression	Numerical value if $\Sigma_t = 1$
$\langle s \rangle_{sp_3}$	$\frac{1.042533}{\Sigma_t}$	1.0425
$\langle s^2 \rangle_{sp_3}$	$\frac{2}{\Sigma_t^2}$	2
$\langle s^3 \rangle_{sp_3}$	$\frac{5.94625}{\Sigma_t^3}$	5.9462
$\langle s^4 \rangle_{sp_3}$	$\frac{24}{\Sigma_t^4}$	24
$\langle s^5 \rangle_{sp_3}$	$\frac{120.734028}{\Sigma_t^5}$	120.7340
$\langle s^6 \rangle_{sp_3}$	$\frac{720}{\Sigma_t^6}$	720

Then, Equations (67) become

$$A\prime^{+}a^{+} + A\prime^{-}a^{-} = -b, \tag{69a}$$

$$A\prime^{+} + A\prime^{-} = 2(1+b)/z_1. \tag{69b}$$

Finally, we solve this system to obtain

$$A^{-} = \gamma^{-}\frac{\langle s \rangle^2}{\langle s^2 \rangle}, \tag{70a}$$

$$A^{+} = \gamma^{+}\frac{\langle s \rangle^2}{\langle s^2 \rangle}, \tag{70b}$$

where

$$\gamma^{-} = 3\frac{2a^{+}(1+b)/z_1 + b}{a^{+} - a^{-}}, \tag{71a}$$

$$\gamma^{+} = 3\frac{2a^{-}(1+b)/z_1 + b}{a^{-} - a^{+}}. \tag{71b}$$

The Green's function we seek is given by

$$G^{\Phi}_{sp_3}(s) = \frac{1}{4\pi s}\frac{\langle s \rangle}{\langle s^2 \rangle}\left[\gamma^{+}\mathrm{e}^{-\alpha^{+}s} + \gamma^{-}\mathrm{e}^{-\alpha^{-}s}\right], \tag{72}$$

and the collision-rate density can be written as

$$f(x) = \int\int\int \frac{1}{4\pi|x-x'|^2}\frac{|x-x'|}{\langle s^2 \rangle}\left[\gamma^{+}\mathrm{e}^{-\alpha^{+}|x-x\prime|} + \gamma^{-}\mathrm{e}^{-\alpha^{-}|x-x\prime|}\right]S(x')dV'. \tag{73}$$

This result agrees with Equation (18) if and only if

$$p(s) = p_{sp_3}(s) := \frac{s}{\langle s^2 \rangle}\left[\gamma^{+}\mathrm{e}^{-\alpha^{+}s} + \gamma^{-}\mathrm{e}^{-\alpha^{-}s}\right]. \tag{74}$$

Although the calculation is not straightforward, $p_{sp_3}(s)$ is always positive and $\int_0^\infty p_{sp_3} ds = 1$, confirming that it defines a probability density function. We can also determine the total cross section, which is written as

$$\Sigma_t(s) = \Sigma_{t,sp_3}(s) := \frac{\frac{s}{\langle s^2\rangle}\left[\gamma^+ e^{-\alpha^+ s} + \gamma^- e^{-\alpha^- s}\right]}{\gamma^+\left(\frac{1}{\alpha^+} + \frac{s}{\langle s^2\rangle}\right)e^{-\alpha^+ s} + \gamma^-\left(\frac{1}{\alpha^-} + \frac{s}{\langle s^2\rangle}\right)e^{-\alpha^- s}}. \tag{75}$$

The nonclassical Equations (1) and (18) with $p(s) = p_{sp_3}(s)$ and $\Sigma_t(s) = \Sigma_{t,sp_3}(s)$ reproduce the Nc-SP$_3$ equations. We can calculate the m^{th} raw moments of $p_{sp_3}(s)$:

$$\langle s^m\rangle_{sp_3} := \int_0^\infty s^m p_{sp_3}(s)ds = \frac{(m+1)!}{\langle s^2\rangle}\left[\frac{\gamma^+}{(\alpha^+)^{(m+2)}} + \frac{\gamma^-}{(\alpha^-)^{(m+2)}}\right]. \tag{76}$$

If classical transport takes place, the moments in Table 1 hold and

$$p_{sp_3}(s) = \Sigma_t^2 s(5.642025e^{-2.94134\Sigma_t s} + 0.469086e^{-1.161256\Sigma_t s}), \tag{77}$$

which is the probability function derived in (Frank et al. 2015) for the SP$_3$ equations (15). The total cross section becomes

$$\Sigma_{t,sp_3}(s) = \frac{5.642025\left(\Sigma_t^2 s\right)e^{-2.94134\Sigma_t s} + 0.469086\left(\Sigma_t^2 s\right)e^{-1.161256\Sigma_t s}}{5.642025\left(\frac{1+2.94134\Sigma_t s}{8.651481}\right)e^{-2.94134\Sigma_t s} + 0.469086\left(\frac{1+1.161256\Sigma_t s}{1.348515}\right)e^{-1.161256\Sigma_t s}}. \tag{78}$$

Table 4 presents the classical expressions for the moments of $p_{sp_3}(s)$, as well as numerical values for $\Sigma_t = 1$. The nonclassical expressions are not explicitly given, but can be obtained from Equation (76); they are consistent with the classical expressions. Comparing to the corresponding classical transport moments in Table 1, the moments are preserved more accurately than in the previous cases (SP$_{1,2}$). In particular, the second, fourth, and sixth moments are exactly preserved as expected. However, these moments are *not* generally preserved in the nonclassical case.

Sampling of s is given by

$$\xi = \int_0^s p(s')ds' = \frac{\gamma^+}{(\alpha^+)^2}\left[1 - (1+\alpha^+ s)e^{-\alpha^+ s}\right] + \frac{\gamma^-}{(\alpha^-)^2}\left[1 - (1+\alpha^- s)e^{-\alpha^- s}\right] = F(s), \tag{79}$$

such that

$$s = F^{-1}(\xi). \tag{80}$$

In the classical case, this expression becomes

$$F(s) = \frac{5.642025}{8.651481}\left[1 - (1 + 2.94134\Sigma_t s)e^{-2.94134\Sigma_t s}\right] \tag{81}$$

$$+\frac{0.469086}{1.348515}\left[1-(1+1.161256\Sigma_t s)\mathrm{e}^{-1.161256\Sigma_t s}\right]. \quad (82)$$

5. Numerical results

This section gives numerical validation for the theoretical results presented in this paper, as well as in references (Frank et al. 2015; Vasques 2016). Specifically, we use a Monte Carlo (MC) *transport* code in which the free-paths were sampled from the probability density functions derived in Section 4. The results of this MC transport code are then compared against the results obtained by deterministically solving the corresponding classical or nonclassical simplified P_N equations. It is important to note that we are *not* concerned about obtaining the correct transport solution of these problems. Our goal is to show that the nonclassical MC transport code correctly reproduces the solutions of the deterministic simplified P_N equations.

Due to the challenges of estimating the free-path distribution $p(s)$ in multi-dimensional nonclassical systems, this task will be left for future work. In this paper, we consider only one-dimensional (1-D) slab geometry transport. Two types of problems have been analyzed: (I) classical transport, and (II) nonclassical transport in an ensemble-averaged (homogenized) periodic random medium. For each of these cases, we have simulated two different internal source configurations: (A) a homogeneous source throughout the whole system (global source); and (B) a constant source located in a small region in the center of the system (local source).

Sections 5.1–5.4 describe each set of problems and present the results obtained. All problems obey the following simplifying assumptions:

- Transport takes place in slab geometry.
- Transport is monoenergetic and scattering is isotropic.
- The source Q emits particles isotropically.
- There are no incoming particles through the boundaries of the system; that is, vacuum boundary conditions.

5.1 Problem set I.A: classical transport, global source

Consider a slab with dimensions $-50 \leq x \leq 50$ composed of a homogeneous material with $\Sigma_t = 1$. We assume that there is a homogeneous source $Q = 1$ throughout the whole system. Under these assumptions, Equation (3) holds and the classical SP_N equations apply. In a diffusive system, it is expected that the scalar fluxes obtained from solving SP_1

COLOR Online / B&W in Print

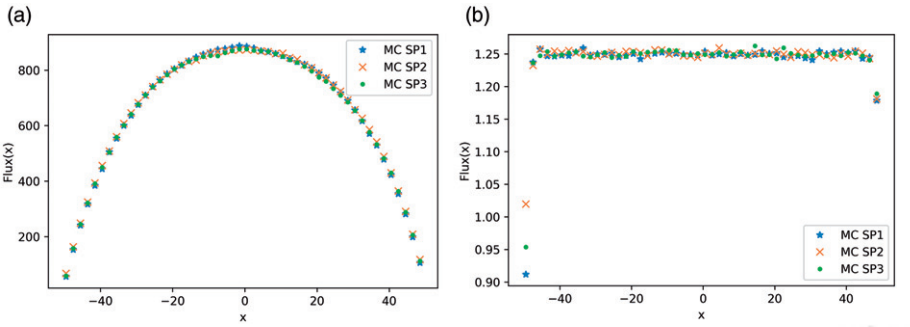

Figure 1. MC simulations for classical transport with global homogeneous source.

[Equation (13)], SP_2 [Equation (14)], and SP_3 [Equations (15)] will converge to the same value, which should approximate the scalar flux obtained from the solution of Equation (4). As the system becomes less diffusive, the scalar flux away from the boundaries should converge to the "infinite solution" $\Phi(x) = Q/[(1-c)\Sigma_t]$.

This can be seen in Figure 1, in which we present results of the simulations performed with the nonclassical MC transport code. We sample the free-paths from Equation (29) (MC SP_1), Equation (47) (MC SP_2), and Equation (77) (MC SP_3). For the diffusive system with $c = 0.999$, the SP_N solutions converge to the same estimate of the scalar flux (Figure 1a). For the system with $c = 0.2$, the SP_N solutions converge to $\Phi(x) = 1/(1-0.2) = 1.25$, as expected (Figure 1b).

Figure 2 is a summary of the results obtained for this set of problems showing estimates for the scalar flux at $x = 0$ for different values of c. The system varies from diffusive to absorbing, and the results of the MC transport code (MC $SP_{1,2,3}$) match those obtained by deterministically solving the SP_N equations ($SP_{1,2,3}$). This is as expected; however, since the solutions of the different equations overlap, this set of results does not provide by itself an appropriate validation of the theoretical predictions.

COLOR Online / B&W in Print

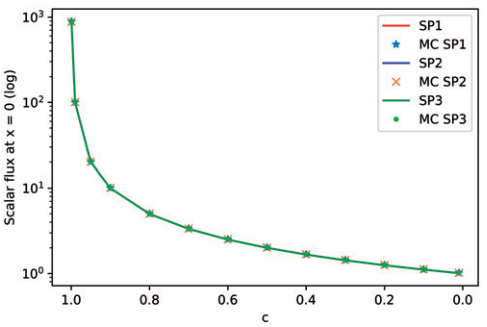

Figure 2. MC and deterministic estimates for the scalar flux (in log) at $x = 0$: problem set I.A.

5.2 Problem set I.B: classical transport, local source

Consider a slab composed of a homogeneous material with $\Sigma_t = 1$. We assume a constant source defined in a region of the system such that

$$Q(x) = \begin{cases} 1, & \text{for } -0.5<x<0.5 \\ 0, & \text{elsewhere.} \end{cases} \tag{83}$$

We allow the system dimensions to be as large as needed in order for the leakage to be negligible. This means that dimensions will increase as c increases and the system becomes more diffusive.

As in the previous case, Equation (3) holds and the classical SP_N equations apply. If the system is diffusive, we expect that the scalar fluxes will approximate the scalar flux obtained from the solution of Equation (4). However, as the system becomes less diffusive, the SP_N equations should yield different results.

Figure 3 shows the results of the simulations performed with the nonclassical MC transport code. Once again, for the diffusive system with $c = 0.999$, the SP_N solutions converge to the same estimate of the scalar flux (Figure 3a). However, we can see that the SP_N solutions yield different results for nondiffusive systems as depicted in Figure 3b.

Figure 4 is a summary of the results obtained for this set of problems. It shows estimates for the scalar flux at $x = 0$ for different values of c. In particular, we see that the MC transport code (MC $SP_{1,2,3}$) accurately matches the solutions obtained by solving the SP_N equations ($SP_{1,2,3}$) deterministically. This validates the theoretical predictions for the classical SP_N transport representations originally introduced in (Frank et al. 2015).

5.3 Problem set II.A: nonclassical transport, global source

We consider a random periodic system as depicted in Figure 5. It represents a random segment of a periodic medium with a period $\ell = 1.0$, containing alternate layers of material 1 (solid) with thickness $\ell_1 = 0.5$, and material 2 (void) with thickness $\ell_2 = 0.5$. Thus, the probability to find material $i = 1, 2$ in position x is given by $P_i = \ell_i/\ell = 1/2$.

Let us assume that this random periodic segment has dimensions $-50 \leq x \leq 50$, and that material 1 is a homogeneous solid with $\Sigma_t = 1$. We also assume that there is a homogeneous source $Q = 1$ throughout the whole system. Under these assumptions, the free-path distribution in the ensemble-averaged (homogenized) system is *not* and exponential. We can numerically estimate the moments of this homogenized angular-dependent free-path distribution; these are given in Table 5. For this class of problems we must apply the Nc-SP_N equations using the estimated moments given in Table 5.

COLOR Online / B&W in Print

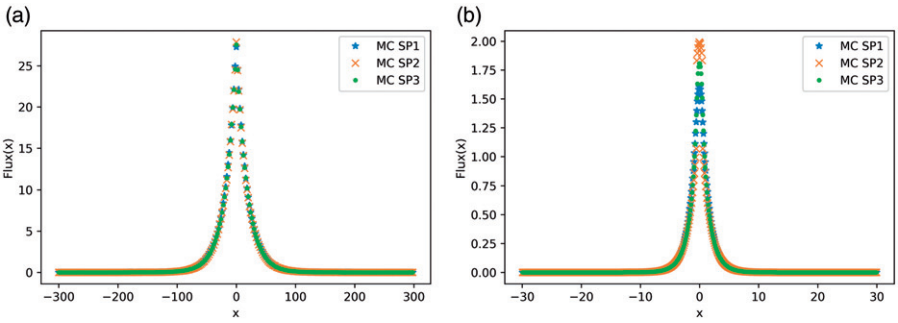

Figure 3. MC simulations for classical transport with constant local source.

COLOR Online / B&W in Print

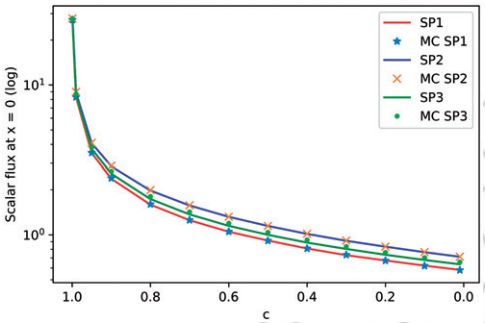

Figure 4. MC and deterministic estimates for the scalar flux (in log) at $x = 0$: problem set I.B.

Figure 5. Sketch of the random periodic medium.

Table 5. Estimated moments of the free-path distribution in the homogenized random periodic medium.

$\langle s \rangle$	$\langle s^2 \rangle$	$\langle s^3 \rangle$	$\langle s^4 \rangle$	$\langle s^5 \rangle$	$\langle s^6 \rangle$
2.000467	8.791506	56.152561	457.65052	4521.87604	52969.8811

COLOR Online / B&W in Print

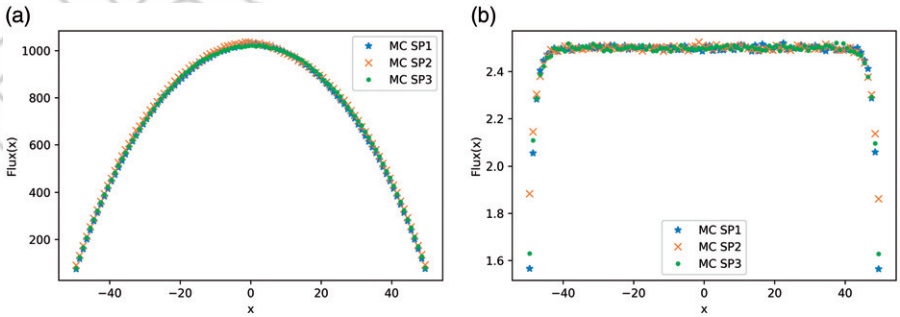

Figure 6. MC simulations for nonclassical transport with global homogeneous source.

Similarly to the results in Section 5.1, it is expected that in a diffusive system the scalar fluxes obtained from solving Nc-SP$_1$ [Equation (8)], Nc-SP$_2$ [Equation (9)], and Nc-SP$_3$ [Equations (11)] will converge to the same value, which should approximate the scalar flux obtained from the solution of Equation (1). As the system becomes less diffusive, the scalar flux away from the boundaries should converge to the volume-averaged infinite solution $\Phi(x) = Q/[(1-c)P_1\Sigma_t]$.

This can be seen in Figure 6, in which we present results of the simulations performed with the nonclassical MC transport code. We sample the free-paths from Equation (26) (MC SP$_1$), Equation (44) (MC SP$_2$), and Equation (74) (MC SP$_3$). For the diffusive system with $c = 0.999$, the Nc-SP$_N$ solutions converge to the same estimate of the scalar flux (Figure 6a). For the system with $c = 0.2$, the Nc-SP$_N$ solutions converge to $\Phi(x) = 1/[(1-0.2)0.5] = 2.5$, as expected (Figure 6b).

Figure 7 is a summary of the results obtained for this set of problems, showing estimates for the scalar flux at $x = 0$ for different values of c. As in the classical case, the MC transport code (MC SP$_{1,2,3}$) closely agrees with the deterministic solutions of the Nc-SP$_N$ equations (SP$_{1,2,3}$).

5.4 Problem set II.B: nonclassical transport, local source

Assume a slab composed of a random segment of the periodic medium described in Section 5.3. We consider a constant source defined in a region of the system such that

$$Q(x) = \begin{cases} 1, & \text{for } -0.5 < x < 0.5 \\ 0, & \text{elsewhere.} \end{cases} \tag{84}$$

As in Section 5.2, we allow the system dimensions to be as large as needed in order for the leakage to be negligible.

We expect the Nc-SP$_N$ equations to yield similar results when the system is diffusive. This can be seen in Figure 8a. As c decreases, the solutions of the Nc-SP$_N$ equations differ, as depicted in Figure 8b. Figure 9 presents a summary of the results obtained for this set of problems, in which it is clear that the MC transport code (MC SP$_{1,2,3}$) closely reproduces the deterministic solutions of the Nc-SP$_N$ equations (SP$_{1,2,3}$).

We note that the MC estimates for the Nc-SP$_3$ solutions present relative errors of 4–5% for a few cases. This is mainly due to the numerical and statistical errors introduced in the MC calculations by numerically estimating the moments in Table 5. Nevertheless, it is clear that the MC simulations predict the overall behavior of the Nc-SP$_3$ equations. These numerical results validate the original theory derived in this paper, demonstrating that

COLOR Online / B&W in Print

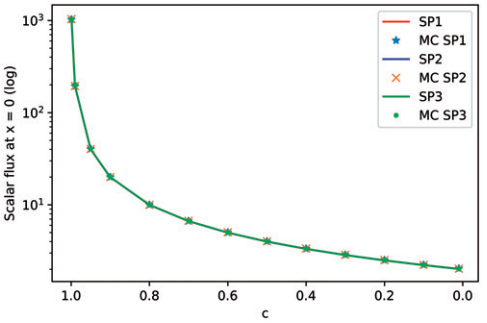

Figure 7. MC and deterministic estimates for the scalar flux (in log) at $x = 0$: problem set II.A.

COLOR Online / B&W in Print

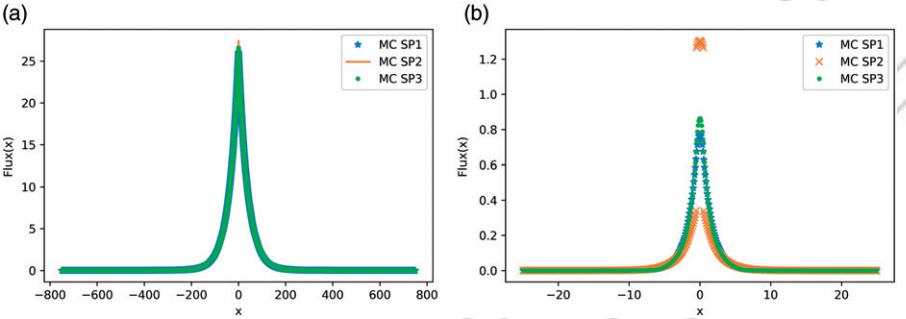

Figure 8. MC simulations for nonclassical transport with constant local source.

COLOR Online / B&W in Print

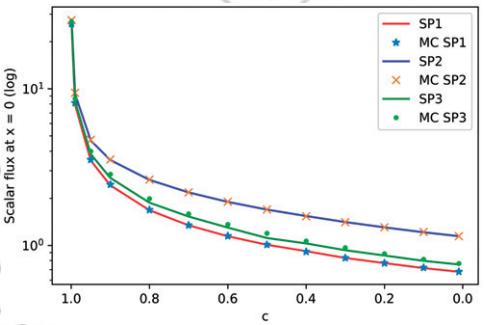

Figure 9. MC and deterministic estimates for the scalar flux (in log) at $x = 0$: problem set II.B.

the nonclassical transport equation (1) can exactly represent the Nc-SP_N equations.

6. Discussion

In this paper, we have shown that the nonclassical simplified $P_{1,2,3}$ equations (Nc-$SP_{1,2,3}$) can be represented exactly by the nonclassical transport equation (1). We derived an explicit expression for the free-path distribution $p(s)$ for each of these equations, and showed that these expressions are a generalization of the ones previously obtained for the classical $SP_{1,2,3}$

equations. We have shown that the moments of the transport $p(s)$ are approximated with increasing accuracy as the order N increases, with the even moments up to $2N$ being preserved when $p(s)$ is exponential.

Moreover, we present numerical simulations that validate our theoretical predictions as well as those presented in previous work (Frank et al. 2015; Vasques 2016). We show that a nonclassical Monte Carlo *transport* code that samples the free-paths from nonexponential distributions can accurately reproduce the deterministic solutions of the Nc-SP_N equations and the classical SP_N equations. This has not been done before.

Although performed only in slab geometry, these numerical results pave the road to consistently simulate these diffusion-based approximations using a Monte Carlo transport method. Furthermore, it hints to the possibility of using these analytical formulations of $p(s)$ to approximate the solutions of the nonclassical Boltzmann equation in near-diffusive systems. Further work needs to be done to investigate how well this approach performs in multi-dimensional nonclassical systems. However, this task must be left for future work.

Acknowledgments

The statements, findings, conclusions, and recommendations are those of the authors and do not necessarily reflect the view of the U.S. Nuclear Regulatory Commission.

Disclosure statement

Q1 No potential conflict of interest was reported by the authors.

Funding

R. Vasques acknowledges support under award number NRC-HQ-84-15-G-0024 from the Nuclear Regulatory Commission. R.N. Slaybaugh acknowledges support under award number NRC-HQ-84-14-G-0052 from the Nuclear Regulatory Commission.

References

Davis, A. B., and A. Marshak. 2010. Solar radiation transport in the cloudy atmosphere: a 3D perspective on observations and climate impacts. *Rep. Prog. Phys.* 73:026801.

d'Eon, E. 2013. Rigorous asymptotic and moment-preserving diffusion approximations for generalized linear Boltzmann transport in arbitrary dimension. *Trans. Theory Stat. Phys.* 42:237–297.

Frank, M., K. Krycki, E.W. Larsen, and R. Vasques. 2015. The nonclassical Boltzmann equation and diffusion-based approximations to the Boltzmann equation. *SIAM J. Appl. Math.* 75:1329–1345.

Gelbard, E. M. 1960. Applications of spherical harmonics method to reactor problems. Technical Report WAPD-BT-20, Bettis Atomic Power Laboratory.

Gelbard, E. M. 1961. Simplified spherical harmonics equations and their use in shielding problems. Technical Report WAPD-T-1182, Bettis Atomic Power Laboratory.

Gelbard, E. M. 1962. Applications of simplified spherical harmonics equations in spherical geometry", Technical Report WAPD-TM-294, Bettis Atomic Power Laboratory.

Larsen, E. W. 2007. A generalized Boltzmann equation for non-classical particle transport. Paper presented at the Proceedings of the Joint International Topical Meeting on Mathematics & Computation and Supercomputing in Nuclear Applications, Monterey, CA, April. 15–19.

Larsen, E.W., and R. Vasques. 2011. A generalized linear boltzmann equation for non-classical particle transport. *J. Quantitat. Spectroscopy Radiat. Trans.* 112:619–631.

Larsen, E. W., J. E. Morel, and J. M. McGhee. 1993. Asymptotic derivation of the simplified PN equations. Paper presented at the Proceedings of the ANS Topical Meeting on Mathematical Methods and Supercomputing in Nuclear Applications, Karlsruhe, Germany, April 19–23, 2.

McClarren, R. G. 2011. Theoretical aspects of the simplified *Pn* equations. *Trans. Theory Stat. Phys.* 39:73–109.

Vasques, R. 2016. The nonclassical diffusion approximation to the nonclassical linear Boltzmann equation. *Appl. Math. Lett.* 53:63–68.

Vasques, R., and E. W. Larsen. 2014. Non-classical particle transport with angular-dependent path-length distributions. II: application to pebble bed reactor cores. *Ann. Nucl. Energy* 70:301–311.

Vasques, R., and R. N. Slaybaugh. 2017. Simplified PN equations for nonclassical transport with isotropic scattering. Paper presented at the Proceedings of the International Conference on Mathematics and Computational Methods Applied to Nuclear Science & Engineering – M&C, Jeju, Korea, April 16–20.